Analysis of *Ustilago maydis pot1* reveals context-dependent, dichotomous regulation of homology-directed DNA repair factors by a telomere protein

Authors

Syed S. Zahid[1], Sarah Aloe[1], Jeanette Sutherland[1], William K. Holloman[1], Neal F. Lue [1, 2] *

[1]Department of Microbiology & Immunology, W. R. Hearst Microbiology Research Center, Weill Cornell Medicine, 1300 York Avenue, New York, New York, 10065, United States of America

[2]Sandra and Edward Meyer Cancer Center, Weill Cornell Medicine, 1300 York Avenue, New York, New York, 10065, United States of America

* To whom correspondence should be addressed. Tel: +1 212 746-6506; Fax: +1 212 746-8587; Email: nflue@med.cornell.edu

Running Title: *U. maydis* Pot1 regulates telomere replication and HDR

Abstract

The telomere G-strand binding protein Pot1 plays multifaceted roles in telomere maintenance and protection. We examined the biochemical activity and genetic mechanisms of Pot1 in *Ustilago maydis*, a fungal model that recapitulates key features of mammalian telomere regulation. We found that *U. maydis* Pot1 binds directly to Rad51 and regulates the latter's strand exchange activity. Deleting an N-terminal domain of Pot1 implicated in Rad51-binding caused telomere shortening, suggesting that Pot1-Rad51 interaction facilitates telomere replication. Depleting Pot1 through transcriptional repression triggered growth arrest as well as rampant recombination, leading to multiple telomere aberrations. In addition, telomere repeat RNAs transcribed from both the G- and C-strand were dramatically up-regulated, and this was accompanied by elevated levels of telomere RNA-DNA hybrids. Telomere abnormalities of *pot1*-deficient cells were suppressed, and cell viability was rescued by the deletion of *rad51* or *brh2* (the *BRCA2* ortholog), indicating that homology-directed repair (HDR) proteins are key mediators of telomere aberrations and cellular toxicity. Together, these observations underscore the complex physical and functional interactions between Pot1 and DNA repair factors, leading to context-dependent and dichotomous effects of HDR proteins on telomere maintenance and protection.

Introduction

A key function of telomeres is to prevent chromosome ends from being recognized as double strand breaks (DSBs); erroneous recognition of telomeres as DSBs leads to the activation of DNA damage response (DDR), resulting in detrimental DNA repair (i.e., non-homologous end joining (NHEJ) or homology-directed repair (HDR)) that engenders chromosomal re-arrangements (1,2). This protective function of telomeres is largely mediated by the shelterin complex, a six-protein assembly that coats double-stranded telomere DNA repeats as well as the terminal 3' overhang (G-overhang) (1). Among the components of shelterin are proteins that directly recognize double-stranded telomere DNA (TRF1 and TRF2), one that recognizes the G-overhang (POT1), and several associated and bridging factors (RAP1, TIN2, and TPP1). The mechanisms by which shelterin components suppress DDR signaling and DNA repair pathways and the division of labor between these components remain central questions in telomere research.

The second key function of telomeres is to promote the retention and replenishment of telomere DNA, which is subject to two types of erosion mechanisms: 1) erosion due to the failure of replication forks to efficiently traverse the G/C-rich telomere repeats; and 2) erosion due to the failure of lagging strand DNA synthesis to copy the parental DNA strand in its entirety ("end replication problem"). This DNA maintenance function of telomeres is also partly mediated by shelterin. However, in contrast to the protective function, which entails suppression of DNA repair, the DNA maintenance function often entails positive regulation of DNA repair factors or polymerases by shelterin components. For example, TPP1 serves a critical function in recruiting telomerase, a special reverse transcriptase that compensates for telomere loss by extending the G-strand (3-5). Similarly, mammalian TRF1 is believed to recruit the BLM helicase to telomeres to help unwind G-rich secondary structures, thereby promoting replication fork progression (6). Thus, shelterin components evidently regulate the DNA repair machinery in a context-dependent manner in order to mediate both telomere protection and telomere maintenance. Understanding the molecular basis of such dichotomous regulation remains a major challenge in telomere research.

The G-strand binding protein Pot1 is one component of shelterin that plays multi-faceted roles in telomere protection and telomere DNA maintenance. Regarding telomere protection, current evidence indicates that mammalian POT1 selectively represses ATR signaling as well as abnormal telomere repair, including HDR and alternative NHEJ (a-NHEJ) (7-11). However, in fission yeast, the loss of *Pot1* leads to rapid telomere loss, culminating eventually in the circularization of chromosomes through NHEJ (12,13). Why the loss of Pot1 results in disparate outcomes is not well understood. POT1 orthologs have also been implicated in telomere DNA maintenance. Mouse POT1b (one of the two POT1 homologs in this organism) interacts with the cognate CTC1-STN1-TEN1 complex (CST) to promote telomere lagging strand synthesis and maturation (14). CST is another widely conserved telomere complex that promotes telomere maintenance in parallel with shelterin by regulating primase-

Pol α (15-17). Additionally, human POT1 mutations that disrupt the POT1-CST interaction also trigger telomere replication defects (18).

An attractive model for dissecting the interplay between telomere proteins and DNA repair factors is the yeast-like basidiomycete fungus *Ustilago maydis*, originally developed by Robin Holliday to investigate recombinational repair (19). In comparison to budding and fission yeasts, *U. maydis* bears greater resemblances to mammalian cells with respect to the telomere and HDR repair machinery, suggesting that it may be a more accurate model for mammalian telomere regulation (20,21). Indeed, we showed that several repair proteins in *U. maydis* promote telomere replication and telomere recombination just like their mammalian orthologs (22-24). Accordingly, we have taken advantage of *U. maydis* to examine the mechanisms and regulation of repair proteins at telomeres (22-25). In one of the published studies, we show that the two double strand telomere binding proteins in *U. maydis*, named Tay1 and Trf2, play distinct roles in telomere maintenance and protection. Tay1, in particular, physically interacts with the Blm helicase and acts in conjunction with the latter to promote telomere replication, providing one illustration of the significance of telomere-repair protein interactions (26).

Herein we report our investigation of *U. maydis* Pot1, the conserved and essential G-strand binding protein. Our data revealed multi-faceted, Pot1-dependent effects of DNA repair factors on telomere regulation. Specifically, we showed that Pot1 binds directly to the core HDR protein Rad51 and regulates the strand exchange activity of Rad51. Deleting an N-terminal region of Pot1 involved in Rad51-binding caused telomere shortening, suggesting that Pot1 positively regulates the telomere replication function of Rad51. However, when Pot1 is depleted through transcriptional repression and telomeres become deprotected, Rad51 and Brh2 act to instigate aberrant repair and the production of abnormal telomere structures, including high levels of telomere repeat-containing non-coding RNAs (i.e., TERRA and its complement). Thus, Pot1 also negatively regulates the activities of Rad51 and Brh2 to suppress telomere instability. <u>Together, these findings demonstrate how a single telomere protein can regulate the HDR machinery in disparate manners in the contexts of normal and deprotected telomeres.</u>

Materials and Methods

Ustilago maydis strains and growth conditions

Standard protocols were employed for the genetic manipulation of *U. maydis* (27-29). All *U. maydis* strains used in this study were haploid and were derived from the UCM350 background (28,30) and are listed in Supp. Table S1.

The *pot1*^{crg1} strain was constructed by integrating a linearized pRU12-*pot1* plasmid containing fragments that correspond to (1) 700 bp of the *pot1* promoter and (2) the first 700 bp of the *pot1* ORF into the *pot1* genomic locus in UCM350. Briefly, the two *pot1* fragments were generated by PCR using appropriate oligos with flanking restriction enzyme sites (Supp. Table S2), and then cloned together in between the *Nde*I and *Eco*RI sites of pRU12 (31). Correct recombination of *Xba*I treated pRU12-*pot1* into the genomic locus results in the insertion of the *cbx*^{R} marker and the *crg1* promoter precisely adjacent to and upstream of the *pot1* ATG initiation codon. Following transformation, the correct mutant strains were selected on YPA supplemented with carboxin (4 µg/ml) and confirmed by PCR. The strains were grown in YPA (1% yeast extract, 2% peptone, 1.5% arabinose) or YPD (1% yeast extract, 2% peptone, 2% dextrose) to induce or repress *pot1* expression, respectively. The *pot1ΔN*^{crg1} was generated in identical fashion except that nucleotide (nt) 1126 to 1825 of the *pot1* ORF was used in place of the nt 1 to 700 fragment in the cloning of the pRU12-*pot1ΔN* disruption plasmid. The *pot1ΔN* strain was constructed by integrating linearized pCbx-*pot1ΔN*, a derivative of pRU12-*pot1ΔN* that contains (i) a 5' homology region with nt -1400 to -700 of the *pot1* promoter, and (ii) a 3' homology region with nt -700 to -1 of the *pot1* promoter fused to nt 1226 to 1825 of the ORF. The *rad51Δ* and *brh2Δ* disruption cassettes have been described before (23). The *pot1*^{crg1} *rad51Δ* and *pot1*^{crg1} *brh2Δ* mutants were generated by transforming *pot1*^{crg1} with the same *rad51* and *brh2* knockout cassettes as those used for the derivation of the single mutants.

Telomere length and structural analyses

Southern analysis of telomere restriction fragments (TRF Southern) was performed using DNA treated with *Pst*I as described previously (23,25). The blots were hybridized to a cloned restriction fragment containing 82 copies of the TTAGGG repeats. For quantitation, we used the formula mean TRF length = $\Sigma (OD_i \times L_i) / \Sigma (OD_i)$ because the majority of TRF length variation stems from differences in subtelomeric lengths (32,33). The in-gel hybridization assays for detecting ssDNA on the G- and C-strand have also been described (22). STELA for telomeres bearing UT4 subtelomeric elements was performed essentially as reported before (34). To detect telomere-telomere fusions, chromosomal DNA was subjected to PCR using two subtelomeric primers (UT4-F and UT6-F) that are extended by DNA polymerase towards the chromosome ends. The PCR reactions (20 µl) contained 1x Failsafe PreMix H, 0.1 µM each of UT4-F and UT6-F, and 2 U Failsafe™ polymerase; the thermocycling consisted of 36 cycles of 94°C for 30 sec, 63°C for 30 sec, and 72°C for 2 min. The fusion PCR products were detected by Southern using either a UT4 or UT6 subtelomeric probe (26). C-circle and G-circles assays were performed as before except that NxGen® phi29 DNA Polymerase (Lucigen Corp.) were used for rolling circle amplifications (25).

Analysis of telomere repeat-containing RNAs

RNAs were purified from log-phase *U. maydis* cultures using acid phenol extraction (35). For Northern analysis, 3 µg of total RNA were resolved by electrophoresis through a 1.0 % agarose/formaldehyde gel (36). After photography under UV light to visualize ethidium bromide-stained RNAs, the gel contents were transferred to a Hybond-N membrane (GE Healthcare) and hybridization was performed in Church mix using a ^{32}P-labeled single-strand oligonucleotide complementary to the G-strand repeats ($CCCTAA_8$). Following exposure to a phosphor screen, the blot was stripped and first re-probed for the C-strand telomere repeat RNA using ^{32}P-labeled $TTAGGG_8$, and subsequently for 26S rRNA using a PCR fragment (amplified with the UmrRNA_26S_121F and UmrRNA_26S_642R primers (Supp. Table S2)). For dot blot analysis, 0.2 µg of RNAs (untreated or pre-treated with various nucleases) in 10 µl were diluted with 30 µl of RNA incubation/denaturation solution (65.7% formamide, 7.7 % formaldehyde, 1.3x MOPS buffer), heated at 65°C for 5 min, and then cooled on ices. After adding 40 µl of 20x SSC, the entire samples were applied to Hybond-N using a Bio-Dot® Microfiltration Apparatus (Bio-Rad Laboratories, Inc.). After UV crosslinking, the blot was hybridized sequentially to the same probes as those for Northern analysis. For end-point RT-PCR, the RNA samples from acid phenol extraction were first treated with Turbo DNase (Thermo Fisher Inc.). Fifty ng of RNAs were subjected to reverse transcription using Superscript III RT at 55°C for 40 min, followed by heating at 70°C for 15 min to inactivate RT, and then subjected to PCR (33-37 cycles of 95°C for 15 sec, 66°C for 15 sec, and 72°C for 30 sec) with Q5 polymerase (NEB Inc.) and appropriate primers (Supp. Table S2).

Purification of Pot1-FG and truncation variants

To express full length and deletion mutants of *U. maydis* Pot1*,* we amplified the *pot1* open reading frame carrying a C-terminal FLAG tag from genomic DNA by PCR amplification using suitable primer pairs (Supp. Table S2). The PCR fragments were cloned into the pSMT3 vector to enable the expression of His_6-SUMO-Pot1-FG fusion proteins. BL21 codon plus strains bearing the expression plasmids were grown in LB supplemented with kanamycin and induced by IPTG as previously described (25). Each fusion protein was purified by (i) Ni-NTA chromatography, (ii) ULP1 cleavage and, and (iii) anti-FLAG affinity chromatography as previously described.

EMSA Assays

For DNA binding assays, purified Pot1-FG was incubated with 1-10 nM P^{32}-labeled probe and 0.5 µg/µl BSA in binding buffer (25 mM HEPES-KOH, pH 7.5, 5 % glycerol, 3 mM $MgCl_2$, 0.1 mM EDTA, 1 mM DTT) at 22^0C for 15 min, and then subjected to electrophoresis at 0.8 V/cm through a 6 % non-denaturing polyacrylamide gel in 1x TBE, followed by PhosphorImager analysis.

Pull down assays for Pot1-Rad51 and Pot1-brh2 interactions

Pot1-FLAG was immobilized on FLAG affinity resin and incubated with 1 µM purified Rad51 or MBP-Brh2/DSS1 complex at 4°C in FLAG(65) buffer (50 mM Tris-HCl, pH 7.5, 65 mM NaCl, 10 % glycerol, 0.1 % NP-40, 2.5 mM $MgCl_2$, 1 mM DTT). Following incubation with mixing on a rotator at 4°C for 1 h, the beads were washed 4 times with 0.5 ml of the FLAG(100) buffer (same as FLAG(65) except that NaCl is at 100 mM), and then the bound proteins eluted with 60 µl FLAG(150) (same as FLAG(65) except that NaCl is at 150 mM) containing 0.2 mg/ml $FLAG_3$ peptide. The eluates were analyzed by Western Blot using anti-Rad51 or anti-MBP antibodies.

Rad51 strand exchange assays

The assays were modified from published protocols (37,38) and were performed in 15 µl of SE buffer (25 mM Tris.HCl, pH 7.5, 25 mM KCl, 2.4 mM $MgCl_2$, 1 mM DTT, 2 mM ATP) containing 0.25 µM labeled dsDNA (39-mer with the P^{32}-labeled top strand), 0.75 µM unlabeled ssDNA (70-mer complementary to the top strand of the 39-mer), and indicated amounts of Rad51 and Pot1-FG. After 20 min of incubation at 35^{0}C, the reactions were terminated by the addition of 5 µl stop solution (80 mM EDTA, 4 % SDS) containing 0.5 µg/µl proteinase K, and incubated for another 20 min at 35^{0}C. Following the addition of 4 µl loading dye (40% glycerol, 0.25% bromophenol blue, 0.25% xylene cyanol), the samples were analyzed by electrophoresis at 0.8 V/cm through a 10% polyacrylamide gel in 1x TBE, and visualized by PhosphorImager scanning.

Results

*Um*Pot1 physically interacts with Rad51 and stimulates the strand exchange activity of Rad51

As reported previously, like other Pot1 orthologs, *U. maydis* Pot1 contains three OB fold domains and binds with high affinity to the canonical G-strand repeats (25). An unusual feature of *Um*Pot1 is the long N-terminal extension (~ 350 amino acids before the first OB fold) (Supp. Fig. 1a), which is predicted to be largely unstructured (39). To assess the function of this region as well as more conserved domains, we expressed truncation variants of Pot1 and analyzed their G-strand binding activity (Supp. Fig. 1a and 1b). Consistent with results for other Pot1 orthologs, we found that high affinity G-strand-binding was mediated exclusively by the first two OB folds of *U. maydis* Pot1 (OB12; K_d < 1 nM); neither the N-terminal extension nor the third OB fold exhibited any appreciable binding activity (Supp. Fig. 1b).

Since our overall objective in studying *U. maydis* telomeres was to dissect the interplay between telomeres and repair proteins, we screened for potential interactions between Pot1 and DNA repair proteins. Using FLAG-tagged Pot1 in affinity pull down assays, we detected substantial binding of Pot1 to purified Rad51, but not Brh2 (Fig. 1a). This binding is probably direct (i.e., not through contaminating nucleic acids) because the addition of benzonase had no effect (Fig. 1b). We then examined the Rad51-binding activities of different domains of Pot1 and detected significant activity for the N-terminus (N) and the first two OB folds (OB12) of Pot1, but minimal binding for the C-terminal OB fold (OB3) (Supp. Fig. 1c). A Pot1 fragment that spans the N-terminus and OB12 showed stronger binding to Rad51 than either domain alone (Supp. Fig. 1c), further supporting the contributions of both regions to Rad51 interaction.

To determine if Pot1 can modulate the recombination activity of Rad51, we employed an oligonucleotide-based strand exchange assay (37,38). As expected, Rad51 alone catalyzed strand exchange between the duplex and ssDNA substrates in an ATP-dependent manner (Fig. 1c). Interestingly, while Pot1 alone exhibited no strand exchange activity, it stimulated strand exchange by ~ 2-fold in the presence of Rad51 (Fig. 1d). By contrast, the duplex telomere protein Tay1, which does not bind Rad51 (26), had no effect on strand exchange either in the absence or presence of Rad51 (Fig. 1d). We further examined the ability of Pot1 truncation derivatives to stimulate strand exchange, and found that both the N-terminus and OB12 domains were required for stimulation (Supp. Fig. 1d). Together, these results implicate direct Pot1-Rad51 interaction in the stimulatory effect of Pot1.

*Um*Pot1 promotes telomere maintenance

The Pot1-Rad51 interaction suggests that the telomere replication function of Rad51 (23,25) might be regulated by Pot1. To test this idea, we sought to determine the consequence of disrupting this interaction. Because mutating the OB12 domain will likely abrogate DNA-binding and trigger telomere deprotection (making it difficult to

interpret the phenotypes), we deleted just the N-terminus of Pot1 (*pot1ΔN*) and used this allele to replace genomic *pot1* through homologous recombination. The *pot1ΔN* mutant did not exhibit obvious growth defect or UV sensitivity (Fig. 2a), suggesting that telomere protection is intact and Pot1 does not regulate the genome-wide repair function of Rad51. We then examined telomere maintenance of *pot1ΔN* using Southern analysis of telomere restriction fragments (TRF), and detected a moderate telomere length reduction in later passages of the mutant in comparison to the wild type strain (Fig. 2b, streaks 6 and 10). To obtain a more quantitative assessment of telomere lengths, we used STELA (single telomere length analysis) to characterize the subpopulations of telomeres that harbor the UT6 subtelomere sequence (34). Consistent with Southern analysis of TRF lengths, the STELA products in *pot1ΔN* are ~ 200 bp shorter than wild type at streak 10, supporting the notion that Pot1 promotes telomere maintenance (Fig. 2c). To further test the notion that Pot1-Rad51 interaction underpins the replication function of Pot1, we compared the telomeres of the *rad51Δ pot1ΔN* double mutant to those of the single mutants (Supp. Fig. 2). No significant differences were observed, supporting the idea that Rad51 acts in the same pathway as the N-terminus of Pot1 to promote telomere maintenance.

Transcriptional repression of *Um*pot1 triggers severe growth defects and multiple telomere aberrations

We next interrogated the telomere protection function of *U. maydis pot1*. Because deleting this gene is likely to be lethal, we generated a conditional mutant ($pot1^{crg1}$) by replacing the endogenous *pot1* promoter with that from *crg1*, which supports elevated transcription in arabinose-containing media (YPA) but is strongly repressed in glucose-containing media (YPD). To assess the N-terminus of Pot1 in telomere protection, we also substituted the *pot1ΔN* promoter with the *crg1* promoter ($pot1\Delta N^{crg1}$). Both mutants exhibited normal growth in YPA, but suffered dramatic growth defects in YPD, consistent with telomere deprotection (Fig. 3a and Supp. Fig. 3a). Indeed, both mutants became growth arrested in glucose, with $pot1\Delta N^{crg1}$ yielding especially small colonies consistent with accelerated arrest. Analysis of cell morphology revealed cells of varying sizes and shapes (Supp. Fig. 3b), suggesting the arrest can occur in different stages of the cell cycle. This makes *pot1*-deficient cells distinct from several other telomere protein mutants such as *ku70* and *trf2*-deficient cells that show predominantly elongated morphologies consistent with G2/M arrest (22,26).

Analysis of telomere repeat DNAs revealed a multiplicity of defects in both the $pot1^{crg1}$ and $pot1\Delta N^{crg1}$ mutants grown in YPD, but with some notable differences (Fig. 3). First, while the lengths of telomeres (as determined by TRF Southern analysis) became quite heterogenous in both mutants, the overall telomere content was substantially higher in $pot1\Delta N^{crg1}$ (Fig. 3b). The heterogeneous telomere fragments of $pot1^{crg1}$ were detected in the absence of *Pst*I digestion, indicating that they exist as extrachromosomal telomere repeat (ECTR) (Supp. Fig. 3c). Second, while C-circles (a marker of telomere recombination) were found to be elevated in both mutants, the $pot1\Delta N^{crg1}$ mutant also harbored high levels of G-circles (Fig. 3c). Third, while $pot1^{crg1}$ exhibited a modest increase in ssDNA on the C-strand (~10 fold), $pot1\Delta N^{crg1}$ showed instead extremely high levels of ssDNA on the G-strand

(Fig. 3d and 3e). Together, these observations indicate that loss of *pot1* triggers high levels of both telomere recombination and resection, leading to increases in both ds and ss telomere DNA, with much of the DNA in the form of ECTR. In addition, the differences between the telomere aberrations in *pot1*^{crg1} and *pot1ΔN*^{crg1} mutants suggest that even at low protein levels, the residual Pot1 can still alter aberrant DNA repair reaction at telomeres. For example, if Pot1 N-terminus interacts with DNA repair factors to influence resection, the absence of the N-terminus in *pot1ΔN*^{crg1} could result in differential generation of ssDNA as we have observed. In contrast to the drastic increases in abnormal structures associated with telomere recombination and resection, PCR analysis of telomere-telomere fusions revealed only mild inductions in the *pot1*^{crg1} and *pot1ΔN*^{crg1} mutants grown in YPA. The fusion levels were either unaffected or just slightly exacerbated when these mutants were grown in YPD (Supp. Fig. 4). Hence, non-homologous end joining does not appear to be strongly activated by *pot1* deficiency.

Interestingly, even when grown in YPA, *pot1ΔN*^{crg1} exhibited greater telomere length heterogeneity and a modest increase in C-circle levels (Fig. 3a and 3b), suggesting mild telomere de-protection. Because this phenotype was not observed in *pot1ΔN*, it was presumably due to the over-expression of the N-terminally truncated protein. While the underlying mechanism is unclear, it is also consistent with the possibility that the N-terminus of Pot1 might physically or functionally interact with DNA repair factors.

The growth and telomere defects of *pot1*-deficient *Ustilago maydis* are greatly suppressed by deletions of *rad51* and *brh2*

Recent studies in mammalian cells suggest that *pot1* plays an especially prominent role in suppressing homology-directed repair at telomeres (7,9). However, this function does not appear to be well conserved in fission yeast (13). To examine the roles of HDR factors in *pot1*-deficient *U. maydis*, we analyzed the phenotypes of the *pot1*^{crg1} *rad51Δ* and *pot1*^{crg1} *brh2Δ* double mutants. Remarkably, both double mutants showed substantially improved growth and manifested more normal morphology in comparison to *pot1*^{crg} when grown YPD (Supp. Fig. 5a and 5b). Thus, Rad51 and Brh2 are evidently required for the toxicity and growth arrest triggered by *pot1* deficiency, i.e., by mediating aberrant repair. Indeed, analysis of telomere repeat DNAs in the double mutants revealed substantial albeit incomplete suppression of the telomere abnormalities observed in *pot1*^{crg1} when the strains are grown in YPD (Fig. 4). For example, both the abnormally long and short telomere fragments detected in *pot1*^{crg1} are greatly reduced (but not eliminated) in *pot1*^{crg1} *rad51Δ* and *pot1*^{crg1} *brh2Δ* (Fig. 4a). Similarly, the extremely elevated C-strand ssDNA levels are suppressed by ~10 to 20-fold in the double mutants (Fig. 4b). Finally, the levels of C-circles (a marker of telomere recombination) in *pot1*^{crg1} are also reduced by more than 10-fold when either *rad51* or *brh2* is deleted (Fig. 4c). Hence, the two core HDR factors appear to play a pivotal role in generating aberrant telomere structures in the absence of *pot1*. These results are like those observed in *pot1*-deficient mammalian cells (7), supporting the utility of interrogating the *U. maydis* mutants in dissecting the underlying mechanisms.

One other notable result from the ssDNA analysis was the frequent detection of prominent ssDNA signals (both G and C-strand) in the wells for strains bearing either *rad51Δ* or *brh2Δ* mutations regardless of the *pot1* status (Fig. 4b, lanes marked with asterisks). This could be due to the accumulation of replication or recombination intermediates, which are known to manifest slow mobility, and is consistent with a role for Rad51 and Brh2 in promoting telomere replication (23).

Upregulation of telomere-repeat containing RNAs is a cardinal feature of *pot1*-deficient cells

While the observations above implicate Rad51 and Brh2 in promoting aberrant telomere repair in *pot1*-deficient *U. maydis*, the mechanisms by which the various telomere aberrations are produced and how they trigger cell cycle arrest remain incompletely understood. In this regard, it is worth noting that both Pot1 and Rad51 have been linked to the regulation of telomere repeat-containing RNA (TERRA), which is proposed to be a critical determinant of telomere maintenance and stability (40). It should be noted that TERRA generally refers to RNAs synthesized by Pol II from subtelomeric promoters and elongated into the G-strand repeats; most studies to date addressed the roles of this non-coding RNA species at telomeres (41,42). However, RNAs that carry the telomere C-strand repeat, named ARIA, have also been reported in *S. pombe* (43,44). In support of the nexus linking *pot1*, *rad51* and TERRA, POT1 deficiency in human cells was shown to increase TERRA-DNA hybrid formation (7), whereas RAD51 is proposed to directly promote such hybrids through its strand exchange activity (45). These precedents argue that TERRA may participate in the pathways mediated by *pot1*-deficiency and *rad51*/*brh2* deletions.

To characterize the potential involvement of telomere-encoded RNA in our mutant strains, we first analyzed the existence of such RNAs by Northern analysis and found little RNA in wild type cells but high levels of transcripts in *pot1*-deficient mutants. Using strand-specific probes, we showed that RNAs corresponding to both G- and C-strands of telomeres were synthesized in the *pot1* deficient mutant (Fig. 5a and 5b). These transcripts were heterogeneous in size but predominantly short (< 1000 nt). RT-PCR analysis confirmed the upregulation of both G- and C-strand RNAs and further suggests that these RNAs include both the subtelomeric region and telomere repeats (Supp. Fig. 6). For example, the UT6 subtelomeric region can be amplified using cDNA generated by the $CCCTAA_4$ primer, consistent with the existence of G-strand TERRA that spans the subtelomeric-telomeric junction (Supp. Fig. 6, top). Likewise, heterogeneous PCR products were generated when C-strand RNA was reverse transcribed with a UT6 primer and then amplified using forward and reverse primers that anneal to UT6 and telomere repeats, respectively (Supp. Fig. 6, middle). This again implies the existence of C-strand RNAs that span the subtelomeric-telomeric junction. Notably, our data do not exclude the presence of C-strand RNAs that comprise exclusively of just the telomere repeats, called ARIA (44). However, to avoid confusion, we will refer to our C-strand subtelomere-telomere RNAs as C-TERRA. In addition, our data are consistent with the existence of C-strand RNAs that comprise exclusively of subtelomere sequence, named ARRET (Supp. Fig. 6, bottom). Altogether, the Northern and RT-PCR analyses demonstrate that abnormally high levels of RNAs are transcribed from both G-

and C-strands in the setting of *pot1*-deficiency. Although the end-point PCR assays could not provide quantitative assessment of RNA levels, the relative signals suggest that C-TERRA was present at higher levels in the mutant (see below for additional evidence).

We next compared the levels of telomere repeat RNAs in the *pot1* single and double mutants by both Northern and dot blots (Fig. 5a – 5d). Both analyses showed that while there were drastic increases in TERRA and C-TERRA (by > 20-fold) in the *pot1* single mutant, these increases were strongly suppressed by *rad51* and *brh2* deletions (by > 5-fold). Thus, aberrant transcriptions of telomere repeats from both G- and C-strands are also regulated by HDR factors in *pot1*-deficient *U. maydis.* Lastly, we used specific nuclease treatments to assess the potential existence of RNA-DNA hybrids in the acid phenol-extracted nucleic acid preparations (prior to DNase I treatment), which should be enriched for both RNA and RNA-DNA hybrid (Supp. Fig. 7). Interestingly, we found that the G-strand hybridization signals in the *pot1*^{crg1}, *pot1*^{crg1} *rad51Δ*, and *pot1*^{crg1} *brh2Δ* mutants were all substantially reduced by pre-treatment with DNase I, implying that the G-strand DNA: C-TERRA hybrid (hybrid I) represents a substantial fraction of the signals. The signals were also partially sensitive to RNase H cleavage, indicating the presence of the alternative hybrid (C-strand DNA : TERRA; hybrid II). In contrast, the C-strand signals in the dot blot assays were mostly insensitive to either nuclease, suggesting that they were predominantly in the form of ssRNA or RNA-RNA hybrid. Notably, the C-strand RNA in hybrid I should be degraded by RNase H and should render the C-strand dot blot signal RNase H-sensitive if hybrid I is abundant relative to free C-strand RNAs. This not being the case, we are led to the notion that telomere C-strand RNA may be significantly more abundant than G-strand TERRA in the *pot1*^{crg1} mutant, implying differences between these two RNA species with respect to their production or stability.

Discussion

There is growing evidence that HDR factors play multi-faceted and seemingly contradictory roles at telomeres. In the context of normal telomere protection, HDR factors facilitate telomere maintenance by stabilizing stalled forks or promoting repair of truncated telomeres (46). However, when protection is compromised, HDR factors are often responsible for triggering further aberrations and exacerbating genomic instability (9,10). How individual telomere proteins interact physically and functionally with DNA repair factors to achieve context-dependent regulation remains a key area of investigation. In this report, we focus on the interplay between the G-strand binding protein Pot1 and the core HDR factors Rad51 and Brh2/BRCA2 using a fungal model that recapitulates crucial aspects of mammalian telomere regulation. We showed that Pot1 negatively regulates Rad51 and Brh2 to prevent aberrant repair that results in loss of cell viability, but also positively regulates Rad51 activity to promote telomere replication, providing an interesting case study for how a single telomere protein can achieve dual regulation of the same DNA repair factor. We also show that up-regulation of aberrant transcription from both G- and C-strand of telomeres is a consistent consequence of telomere deprotection. The potential mechanisms and implications of these observations are discussed below.

U. maydis Pot1 suppresses the toxic activities of core HDR factors at telomeres

Previous analysis of *S. pombe* Pot1 (*Sp*Pot1) suggests that fungal Pot1 may act differently than the mammalian orthologs in telomere protection: rather than aberrant recombination, loss or inactivation of *Sp*Pot1 leads to rapid telomere resection/loss followed by frequent circularization of chromosomes to stabilize the genome and sustain cell viability (12,13). In contrast, we showed that the phenotypes of *Um*Pot1-deficient cells are very similar to those of comparable mammalian cells, suggesting that suppression of HDR activities may be a widely conserved function of Pot1 in evolution. Importantly, the loss of viability triggered by *U. maydis pot1*-deficiency is almost completely suppressed by *rad51Δ* or *brh2Δ*, confirming the toxicity of HDR factors in the context of telomere dysfunction. This toxicity is at least somewhat specific given that *rad51Δ* fails to ameliorate the telomere toxicity triggered by *ku70* deficiency (22). Instead, the *ku70* deficiency-induced abnormalities are completely suppressed by concurrent *blm* deletion (24). Thus, there is a clear division of labor among telomere proteins in managing aberrant repair. The mechanistic underpinnings for this remain unclear and demands further investigation.

Viewed from another perspective, it is striking that in *U. maydis, ku70* and *pot1* become dispensable for cell viability when specific DNA repair factors are deleted. Such examples of telomere protein dispensability in the context of DNA repair deficiency reify the concept that telomeres have evolved to restrain aberrant repair. It is worth noting that in mammalian cells, there are few examples where the loss of DNA repair factors has been shown to restore the viability of cells missing a key telomere protein. This is probably because mammalian DNA repair factors are often essential for viability in normal mitotic cells. The reduced dependency of *U. maydis* on DNA

repair makes it possible to firmly establish the interconnections between telomere deprotection, aberrant telomere DNA repair, and loss of cell viability.

U. maydis Pot1 promotes telomere maintenance by enhancing the function of Rad51

POT1 has been proposed to promote telomere maintenance in mammalian cells through multiple mechanisms. First, POT1 unwinds G-quadruplexes *in vitro*, and this biochemical activity is thought to facilitate telomerase activity and telomere replication (47,48). Second, POT1 binds to and acts in conjunction with the CST complex to facilitate telomere replication and C-strand fill-in synthesis (14,18). Our analysis of *U. maydis* Pot1 suggests an additional, non-mutually exclusive mechanism, namely through the regulation of Rad51 activity. Notably, while we showed that Pot1 can stimulate the strand exchange activity of Rad51 through direct protein-protein interaction, how this *in vitro* regulation reflects the *in vivo* mechanism of Rad51 at telomeres remains unclear. If Pot1 enhances the formation or stability Rad51 filaments, this could promote complete replication by stabilizing stalled forks. However, it is also clear that rampant strand exchange by Rad51 at telomeres is toxic to the cell and is restrained by Pot1 (see the section above). Thus, it is possible that Pot1-Rad51 interaction may positively regulate some aspects of Rad51 activity while suppressing others in a context dependent manner, e.g., through modulation by other telomere and DNA-repair factors. More studies will be necessary to disentangle the molecular basis of Pot1-mediated regulation of Rad51 in *U. maydis*.

Notably, mammalian RAD51 is also implicated in telomere replication (46), but a direct POT1-RAD51 connection has not been reported. Instead, there is substantial evidence that RAD51 is regulated by CST, the complex that acts in parallel with shelterin to promote telomere maintenance. For example, CST associates with Rad51, and CST deficiency impairs the recruitment of RAD51 to genomic sites of replication stress (49). In addition, CTC1 disease mutations that compromise telomere maintenance often disrupt its association with RAD51 (50). Whether POT1 acts in conjunction or in parallel with CST to regulate RAD51 function at mammalian telomeres are interesting questions for future analysis. Conversely, it will be worthwhile to determine if *U. maydis* CST subunits regulate Rad51 function. However, it should be noted that only Stn1 and Ten1 homologs are readily discernible in the *U. maydis* genome (just like *S. pombe*), suggesting that some fungal lineages may have undergone significant remodeling of the CST complex (23,51).

The existence of both Pot1-Rad51 and CST-RAD51 interactions (albeit in different organisms) also has evolutionary implications. Based on structural and functional considerations, it has been argued that POT1-TPP1 and CST may represent ancient paralogs (i.e., POT1 ≈ CTC1 and TPP1 ≈ STN1), and accordingly may manifest functional overlaps or functional reshuffling in different organisms (17). That both Pot1 and CST protein family members can bind RAD51 provides additional support for this conjecture.

Aberrant transcription of telomere repeats at de-protected telomeres

There is growing evidence that while TERRA is crucial for normal telomere regulation (40,52), it is often aberrantly expressed from damaged telomeres and can promote abnormal telomere metabolism by forming RNA-DNA hybrids or by interacting with a multiplicity of factors (53-56). Of more direct relevance to the current study, the depletion or knockout of shelterin components in both mammals and fungi has been shown to trigger the production of telomere repeat RNAs as well as RNA-DNA hybrids. For example, depleting human TRF2 leads to rampant up-regulation of TERRA, which in turn alters histone methylation and promotes end-to-end fusion (57). Similarly, knocking out human POT1 triggers both abnormal recombination as well as the accumulation of telomere RNA-DNA hybrid (7). Consistent with these precedents, we observed dramatic upregulation of telomere repeat containing RNAs in *pot1*-deficient *U. maydis*. However, both the structure of the RNAs and their relative expression manifest notable features.

One notable feature is the structure of the C-strand RNA. In mammalian cells, this RNA species is evidently expressed at very low levels (if at all) from normal telomeres, and its structure has not been investigated in detail (41,42). In *S. pombe*, the C-strand RNAs are synthesized to some degree from normal telomeres and are dramatically up-regulated in a number of mutants, including *rap1Δ*, *taz1Δ*, and *poz1*Δ (44,58). However, unlike C-TERRA in *U. maydis*, which encompasses both subtelomere and telomere repeats, the *S. pombe* C-strand RNAs are reported to comprise just the telomere repeat (ARIA) or subtelomere regions (ARRET). This discrepancy indicates either there are species-specific differences in the biogenesis of C-strand RNA, or the *S. pombe* ARIA and ARRET could arise through post transcriptional processing. An unresolved conundrum concerning C-strand repeat RNA (ARIA or C-TERRA) is that transcription must initiate within the telomere repeat region, which (unlike subtelomeric Pol II promoters responsible for TERRA transcription) does not contain promoter- or initiator-like elements. Thus, an unusual, promoter-independent mode of RNA synthesis is probably involved. Regardless of the potential mechanisms, our observation suggests that C-strand RNA synthesis may be relatively common at deprotected telomeres and is worthy of further investigation. Conversely, the growing evidence for promiscuous transcription at de-protected telomeres suggests that a key function of telomere proteins is in fact to suppress aberrant transcription.

Another unexpected finding is the greater abundance of C-TERRA relative to TERRA in the *pot1* mutants. As described before, both the RT-PCR and dot blot analyses support the idea that C-TERRA is present at higher levels when *pot1* is depleted (Supp. Fig. 6 and Supp. Fig. 7). Whether this is due to enhanced synthesis or greater stability of the C-strand RNA is unclear. The high levels of C-TERRA may partially account for the formation of hybrid I (G-strand DNA: C-TERRA), which was readily detected in the mutant. Most studies of telomere RNA-DNA hybrid have focused on the roles of hybrid II (C-strand DNA: TERRA) and the associated R-loops, and have

implicated these structures in telomere abnormalities. Our identification of hybrid I uncovers yet another structure that could be responsible for exacerbating telomere damage.

Finding

This work was supported by a pilot project grant from the Sandra and Edward Meyer Cancer Center (N.F.L. and W.K.H.), NSF MCB-1817331, and NIH GM 107287 (N.F.L.).

Conflict of interest

The authors declare no competing interests.

Acknowledgments

We thank Qingwen Zhou for purified Rad51 and Brh2/Dss1, and members of our laboratories for discussion.

Data availability

The data generated and/or analysed during the current study are included within the paper and Supplementary Information or available from the corresponding author upon reasonable request.

References

1. de Lange, T. (2018) Shelterin-Mediated Telomere Protection. *Annu Rev Genet*, **52**, 223-247.

2. Arnoult, N. and Karlseder, J. (2015) Complex interactions between the DNA-damage response and mammalian telomeres. *Nat Struct Mol Biol*, **22**, 859-866.

3. Schmidt, J.C. and Cech, T.R. (2015) Human telomerase: biogenesis, trafficking, recruitment, and activation. *Genes & development*, **29**, 1095-1105.

4. Autexier, C. and Lue, N.F. (2006) The Structure And Function of Telomerase Reverse Transcriptase. *Annu Rev Biochem*, **75**, 493-517.

5. Wu, R.A., Upton, H.E., Vogan, J.M. and Collins, K. (2017) Telomerase Mechanism of Telomere Synthesis. *Annu Rev Biochem*, **86**, 439-460.

6. Zimmermann, M., Kibe, T., Kabir, S. and de Lange, T. (2014) TRF1 negotiates TTAGGG repeat-associated replication problems by recruiting the BLM helicase and the TPP1/POT1 repressor of ATR signaling. *Genes & development*, **28**, 2477-2491.

7. Glousker, G., Briod, A.S., Quadroni, M. and Lingner, J. (2020) Human shelterin protein POT1 prevents severe telomere instability induced by homology-directed DNA repair. *EMBO J*, **39**, e104500.

8. Hockemeyer, D., Sfeir, A.J., Shay, J.W., Wright, W.E. and de Lange, T. (2005) POT1 protects telomeres from a transient DNA damage response and determines how human chromosomes end. *EMBO J*, **24**, 2667-2678.

9. Wu, L., Multani, A.S., He, H., Cosme-Blanco, W., Deng, Y., Deng, J.M., Bachilo, O., Pathak, S., Tahara, H., Bailey, S.M. *et al.* (2006) Pot1 deficiency initiates DNA damage checkpoint activation and aberrant homologous recombination at telomeres. *Cell*, **126**, 49-62.

10. Hockemeyer, D., Daniels, J.P., Takai, H. and de Lange, T. (2006) Recent expansion of the telomeric complex in rodents: Two distinct POT1 proteins protect mouse telomeres. *Cell*, **126**, 63-77.

11. Gu, P., Wang, Y., Bisht, K.K., Wu, L., Kukova, L., Smith, E.M., Xiao, Y., Bailey, S.M., Lei, M., Nandakumar, J. *et al.* (2017) Pot1 OB-fold mutations unleash telomere instability to initiate tumorigenesis. *Oncogene*, **36**, 1939-1951.

12. Baumann, P. and Cech, T.R. (2001) Pot1, the putative telomere end-binding protein in fission yeast and humans. *Science*, **292**, 1171-1175.

13. Pitt, C.W. and Cooper, J.P. (2010) Pot1 inactivation leads to rampant telomere resection and loss in one cell cycle. *Nucleic acids research*, **38**, 6968-6975.

14. Wu, P., Takai, H. and de Lange, T. (2012) Telomeric 3' overhangs derive from resection by Exo1 and Apollo and fill-in by POT1b-associated CST. *Cell*, **150**, 39-52.

15. Lue, N.F., Chan, J., Wright, W.E. and Hurwitz, J. (2014) The CDC13-STN1-TEN1 complex stimulates Pol alpha activity by promoting RNA priming and primase-to-polymerase switch. *Nat Commun*, **5**, 5762.

16. Giraud-Panis, M.J., Teixeira, M.T., Geli, V. and Gilson, E. (2010) CST meets shelterin to keep telomeres in check. *Mol Cell*, **39**, 665-676.

17. Lue, N.F. (2018) Evolving Linear Chromosomes and Telomeres: A C-Strand-Centric View. *Trends Biochem Sci*, **43**, 314-326.

18. Pinzaru, A.M., Hom, R.A., Beal, A., Phillips, A.F., Ni, E., Cardozo, T., Nair, N., Choi, J., Wuttke, D.S., Sfeir, A. *et al.* (2016) Telomere Replication Stress Induced by POT1 Inactivation Accelerates Tumorigenesis. *Cell Rep*, **15**, 2170-2184.

19. Holloman, W.K., Schirawski, J. and Holliday, R. (2008) The homologous recombination system of Ustilago maydis. *Fungal Genet Biol*, **45 Suppl 1**, S31-39.

20. Guzman, P.A. and Sanchez, J.G. (1994) Characterization of telomeric regions from Ustilago maydis. *Microbiology*, **140 (Pt 3)**, 551-557.

21. Holloman, W.K. (2011) Unraveling the mechanism of BRCA2 in homologous recombination. *Nat Struct Mol Biol*, **18**, 748-754.

22. de Sena-Tomas, C., Yu, E.Y., Calzada, A., Holloman, W.K., Lue, N.F. and Perez-Martin, J. (2015) Fungal Ku prevents permanent cell cycle arrest by suppressing DNA damage signaling at telomeres. *Nucleic acids research*.

23. Yu, E.Y., Kojic, M., Holloman, W.K. and Lue, N.F. (2013) Brh2 and Rad51 promote telomere maintenance in Ustilago maydis, a new model system of DNA repair proteins at telomeres. *DNA Repair (Amst)*, **12**, 472-479.

24. Yu, E.Y., Perez-Martin, J., Holloman, W.K. and Lue, N.F. (2015) Mre11 and Blm-Dependent Formation of ALT-Like Telomeres in Ku-Deficient Ustilago maydis. *PLoS Genet*, **11**, e1005570.

25. Yu, E.Y., Hsu, M., Holloman, W.K. and Lue, N.F. (2018) Contributions of recombination and repair proteins to telomere maintenance in telomerase-positive and negative Ustilago maydis. *Mol Microbiol*, **107**, 81-93.

26. Yu, E.Y., Zahid, S.S., Ganduri, S., Sutherland, J.H., Hsu, M., Holloman, W.K. and Lue, N.F. (2020) Structurally distinct telomere-binding proteins in Ustilago maydis execute non-overlapping functions in telomere replication, recombination, and protection. *Commun Biol*, **3**, 777.

27. Kamper, J. (2004) A PCR-based system for highly efficient generation of gene replacement mutants in Ustilago maydis. *Molecular genetics and genomics : MGG*, **271**, 103-110.

28. Kojic, M., Kostrub, C.F., Buchman, A.R. and Holloman, W.K. (2002) BRCA2 homolog required for proficiency in DNA repair, recombination, and genome stability in Ustilago maydis. *Mol Cell*, **10**, 683-691.

29. Brachmann, A., Konig, J., Julius, C. and Feldbrugge, M. (2004) A reverse genetic approach for generating gene replacement mutants in Ustilago maydis. *Molecular genetics and genomics : MGG*, **272**, 216-226.

30. Banuett, F. and Herskowitz, I. (1989) Different a alleles of Ustilago maydis are necessary for maintenance of filamentous growth but not for meiosis. *Proceedings of the National Academy of Sciences of the United States of America*, **86**, 5878-5882.

31. Bottin, A., Kamper, J. and Kahmann, R. (1996) Isolation of a carbon source-regulated gene from Ustilago maydis. *Mol Gen Genet*, **253**, 342-352.

32. Kimura, M., Stone, R.C., Hunt, S.C., Skurnick, J., Lu, X., Cao, X., Harley, C.B. and Aviv, A. (2010) Measurement of telomere length by the Southern blot analysis of terminal restriction fragment lengths. *Nature Protocols*, **5**, 1596-1607.

33. Mender, I. and Shay, J.W. (2015) Telomere Restriction Fragment (TRF) Analysis. *Bio Protoc*, **5**.

34. Swapna, G., Yu, E.Y. and Lue, N.F. (2018) Single telomere length analysis in Ustilago maydis, a high-resolution tool for examining fungal telomere length distribution and C-strand 5'-end processing. *Microb Cell*, **5**, 393-403.

35. Collart, M.A. and Oliviero, S. (1993) Preparation of yeast RNA. *Curr Protoc Mol Biol*, **23**, 13.12.11-13.12.15.

36. Sanchez, A.M., Garg, A., Shuman, S. and Schwer, B. (2019) Inositol pyrophosphates impact phosphate homeostasis via modulation of RNA 3' processing and transcription termination. *Nucleic acids research*, **47**, 8452-8469.

37. Mazloum, N., Zhou, Q. and Holloman, W.K. (2007) DNA binding, annealing, and strand exchange activities of Brh2 protein from Ustilago maydis. *Biochemistry*, **46**, 7163-7173.

38. Rice, K.P., Eggler, A.L., Sung, P. and Cox, M.M. (2001) DNA pairing and strand exchange by the Escherichia coli RecA and yeast Rad51 proteins without ATP hydrolysis: on the importance of not getting stuck. *J Biol Chem*, **276**, 38570-38581.

39. Meszaros, B., Erdos, G. and Dosztanyi, Z. (2018) IUPred2A: context-dependent prediction of protein disorder as a function of redox state and protein binding. *Nucleic acids research*, **46**, W329-W337.

40. Azzalin, C.M. and Lingner, J. (2015) Telomere functions grounding on TERRA firma. *Trends Cell Biol*, **25**, 29-36.

41. Azzalin, C.M., Reichenbach, P., Khoriauli, L., Giulotto, E. and Lingner, J. (2007) Telomeric repeat containing RNA and RNA surveillance factors at mammalian chromosome ends. *Science*, **318**, 798-801.

42. Schoeftner, S. and Blasco, M.A. (2008) Developmentally regulated transcription of mammalian telomeres by DNA-dependent RNA polymerase II. *Nat Cell Biol*, **10**, 228-236.

43. Greenwood, J. and Cooper, J.P. (2012) Non-coding telomeric and subtelomeric transcripts are differentially regulated by telomeric and heterochromatin assembly factors in fission yeast. *Nucleic acids research*, **40**, 2956-2963.

44. Bah, A., Wischnewski, H., Shchepachev, V. and Azzalin, C.M. (2012) The telomeric transcriptome of Schizosaccharomyces pombe. *Nucleic acids research*, **40**, 2995-3005.

45. Feretzaki, M., Pospisilova, M., Valador Fernandes, R., Lunardi, T., Krejci, L. and Lingner, J. (2020) RAD51-dependent recruitment of TERRA lncRNA to telomeres through R-loops. *Nature*, **587**, 303-308.

46. Badie, S., Escandell, J.M., Bouwman, P., Carlos, A.R., Thanasoula, M., Gallardo, M.M., Suram, A., Jaco, I., Benitez, J., Herbig, U. *et al.* (2010) BRCA2 acts as a RAD51 loader to facilitate telomere replication and capping. *Nat Struct Mol Biol*, **17**, 1461-1469.

47. Hwang, H., Buncher, N., Opresko, P.L. and Myong, S. (2012) POT1-TPP1 regulates telomeric overhang structural dynamics. *Structure*, **20**, 1872-1880.

48. Zaug, A.J., Podell, E.R. and Cech, T.R. (2005) Human POT1 disrupts telomeric G-quadruplexes allowing telomerase extension in vitro. *Proceedings of the National Academy of Sciences of the United States of America*, **102**, 10864-10869.

49. Chastain, M., Zhou, Q., Shiva, O., Fadri-Moskwik, M., Whitmore, L., Jia, P., Dai, X., Huang, C., Ye, P. and Chai, W. (2016) Human CST Facilitates Genome-wide RAD51 Recruitment to GC-Rich Repetitive Sequences in Response to Replication Stress. *Cell Rep*, **16**, 1300-1314.

50. Wang, Y. and Chai, W. (2018) Pathogenic CTC1 mutations cause global genome instabilities under replication stress. *Nucleic acids research*, **46**, 3981-3992.

51. Lue, N.F. (2010) Plasticity of telomere maintenance mechanisms in yeast. *Trends Biochem Sci*, **35**, 8-17.

52. Kwapisz, M. and Morillon, A. (2020) Subtelomeric Transcription and its Regulation. *J Mol Biol*, **432**, 4199-4219.

53. Sagie, S., Toubiana, S., Hartono, S.R., Katzir, H., Tzur-Gilat, A., Havazelet, S., Francastel, C., Velasco, G., Chedin, F. and Selig, S. (2017) Telomeres in ICF syndrome cells are vulnerable to DNA damage due to elevated DNA:RNA hybrids. *Nat Commun*, **8**, 14015.

54. Arora, R., Lee, Y., Wischnewski, H., Brun, C.M., Schwarz, T. and Azzalin, C.M. (2014) RNaseH1 regulates TERRA-telomeric DNA hybrids and telomere maintenance in ALT tumour cells. *Nat Commun*, **5**, 5220.

55. Vohhodina, J., Goehring, L.J., Liu, B., Kong, Q., Botchkarev, V.V., Jr., Huynh, M., Liu, Z., Abderazzaq, F.O., Clark, A.P., Ficarro, S.B. *et al.* (2021) BRCA1 binds TERRA RNA and suppresses R-Loop-based telomeric DNA damage. *Nat Commun*, **12**, 3542.

56. Ghisays, F., Garzia, A., Wang, H., Canasto-Chibuque, C., Hohl, M., Savage, S.A., Tuschl, T. and Petrini, J.H.J. (2021) RTEL1 influences the abundance and localization of TERRA RNA. *Nat Commun*, **12**, 3016.

57. Porro, A., Feuerhahn, S., Delafontaine, J., Riethman, H., Rougemont, J. and Lingner, J. (2014) Functional characterization of the TERRA transcriptome at damaged telomeres. *Nat Commun*, **5**, 5379.

58. Lorenzi, L.E., Bah, A., Wischnewski, H., Shchepachev, V., Soneson, C., Santagostino, M. and Azzalin, C.M. (2015) Fission yeast Cactin restricts telomere transcription and elongation by controlling Rap1 levels. *EMBO J*, **34**, 115-129.

Fig. 1

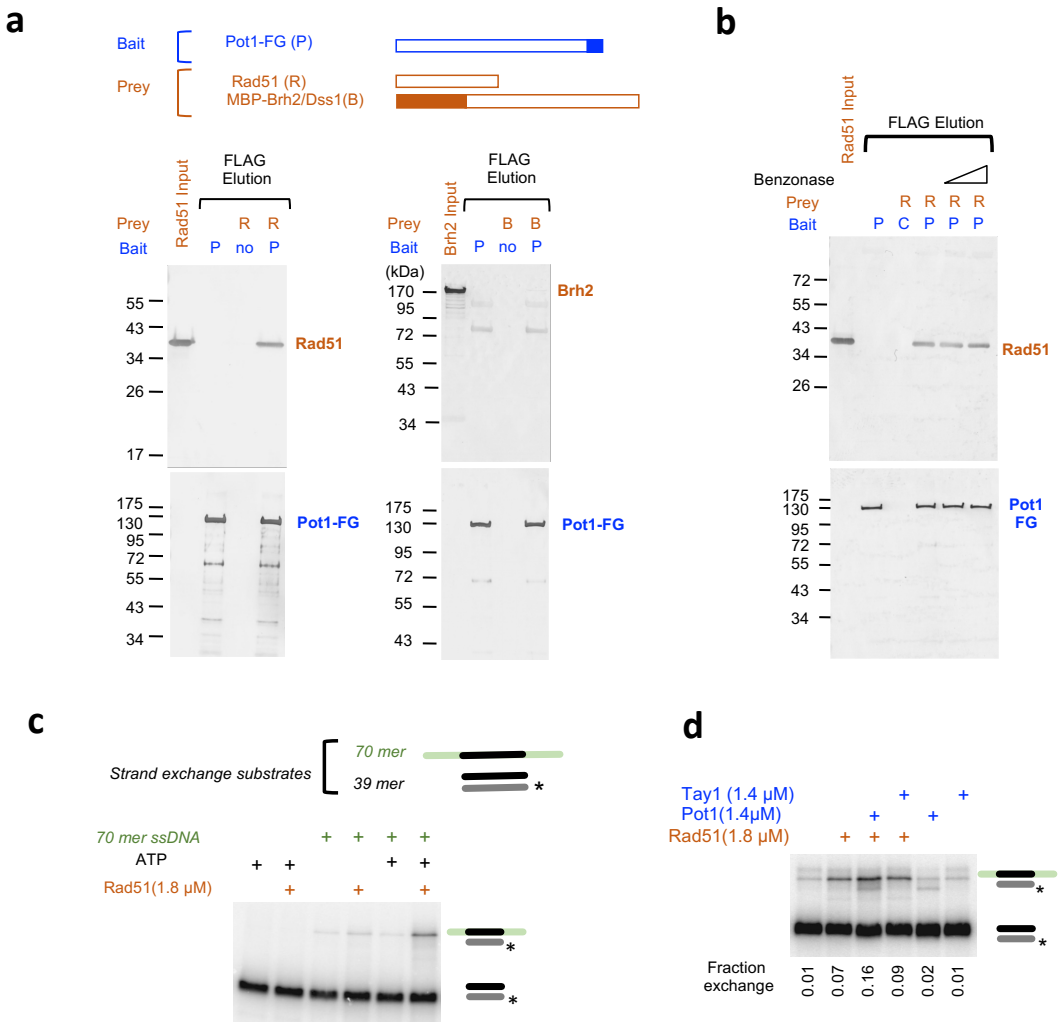

Figure 1. *U maydis* Pot1 binds to Rad51 and regulate the strand-exchange activity of Rad51

a. Anti-FLAG agarose resin was pre-bound with Pot1-FLAG and tested for interaction with purified Rad51 or MBP-Brh2/Dss1 complex. The bound proteins were eluted with $FLAG_3$ peptides and the levels of Rad51, Brh2 and Pot1 in the eluates analyzed using anti-Rad51, anti-MBP, and anti-FLAG antibodies.

b. The interaction between Pot1-FLAG and Rad51 was analyzed in the absence or presence of Benzonase.

c. The ability of Rad51 to mediate strand exchange between a 70-mer ssDNA and a labeled 39-mer dsDNA was analyzed in the absence or presence of ATP.

d. The effects of Pot1 and Tay1 on strand exchange were analyzed in the absence or presence of Rad51.

Fig. 2

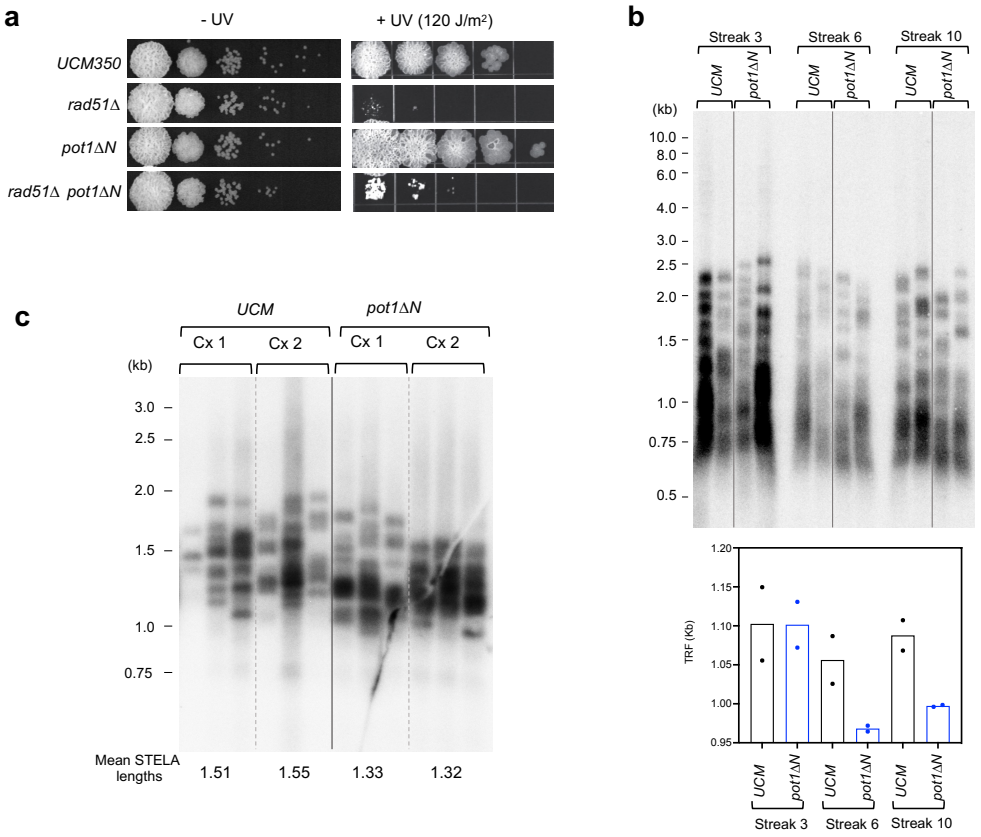

Figure 2. Pot1 N-terminal deletion impairs telomere maintenance

a. Serial dilutions of the indicated *U. maydis* strains were directly spotted onto a YPD plate or first subjected to UV irradiation prior to spotting. The plates were incubated for 2 days (-UV) or 3 days (+UV) and the results photographed.

b. Chromosomal DNAs from two independently propagated clonal cultures of UCM350 and *pot1ΔN* were subjected to TRF Southern analysis at the indicated passages (i.e., Streak 3, 6 and 10). Mean TRF lengths from the pairs of assays were calculated and plotted at the bottom.

c. Chromosomal DNAs from two independently propagated clonal cultures of UCM350 and *pot1ΔN* strains were subjected to STELA analysis at the Streak 10. Mean STELA lengths were calculated from 3 independent assays of each DNA sample and shown at the bottom.

Fig. 3

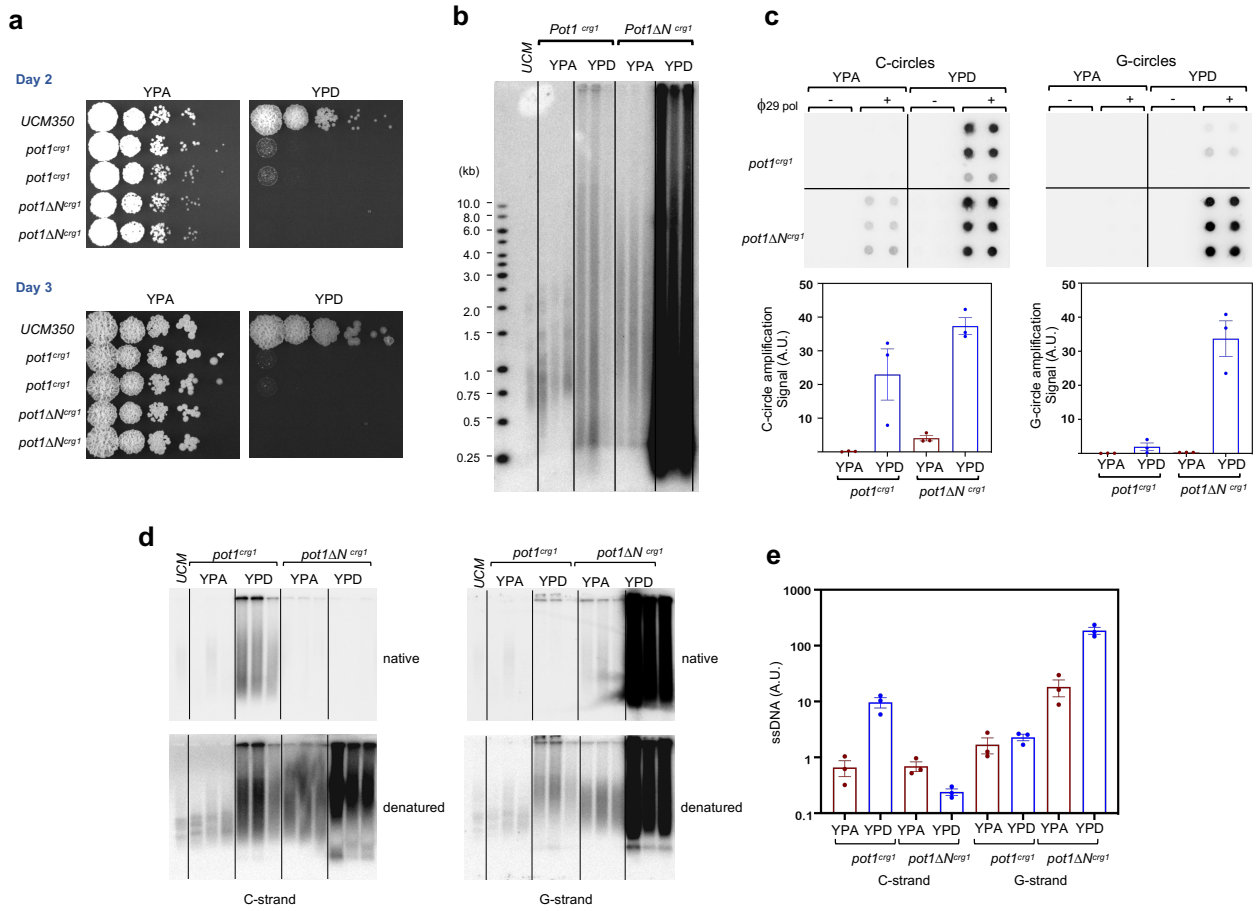

Figure 3. *pot1* deficiency triggers growth arrest and multiple telomere aberrations

a. Serial dilutions of the indicated strains were grown on YPA (*crg1* promoter on) and YPD (*crg1* promoter off) plates for 2 and 3 days, and the results photographed.

b. Chromosomal DNAs from three independently generated *pot1*^{crg1} and *pot1*ΔN^{crg1} strains grown in YPA and YPD were subjected to telomere restriction fragment analysis.

c. Chromosomal DNAs from three independently generated *pot1*^{crg1} and *pot1*ΔN^{crg1} strains grown in YPA and YPD were subjected to C-circle and G-circle assays. The relative levels of C- and G-circles from the three mutants were quantified and plotted at the bottom.

d. Chromosomal DNAs from three independently generated *pot1*^{crg1} and *pot1*ΔN^{crg1} strains grown in YPA and YPD were subjected to in-gel hybridization analysis of ssDNA on both the G- and the C-strand.

e. The levels of ssDNA from the in-gel hybridization assays were quantified (N=3) and plotted.

Fig. 4

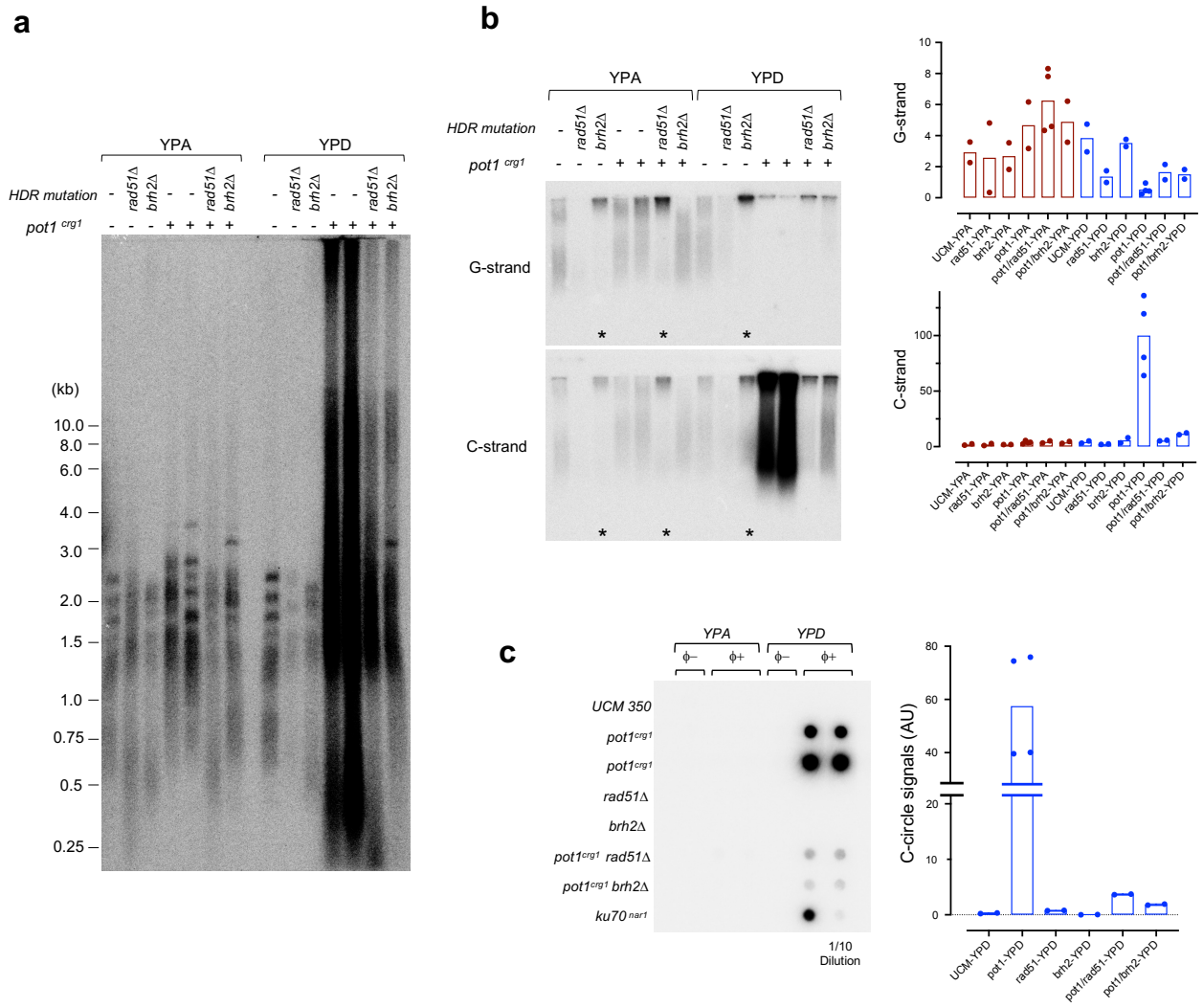

Figure 4. Telomere aberrations in *pot1*-deficient *U. maydis* are greatly suppressed by *rad51*Δ and *brh2*Δ

a. Chromosomal DNAs from the indicated wild type and mutant strains grown in YPA and YPD were subjected to telomere restriction fragment analysis. Two independently generated *pot1*^{crg1} strains were analyzed in all the assays in this figure.

b. Chromosomal DNAs from the indicated wild type and mutant strains grown in YPA and YPD were subjected to subjected to in-gel hybridization analysis of ssDNA on both the G- and the C-strand (left). The levels of ssDNA from two independent sets of assays were quantified and plotted (right).

c. Chromosomal DNAs from the indicated wild type and mutant strains grown in YPA and YPD were subjected to C- and G-circle assays (left). The relative levels of C- and G-circle signals from these strains were quantified and plotted (right). Data are from two independent sets of assays.

Fig. 5

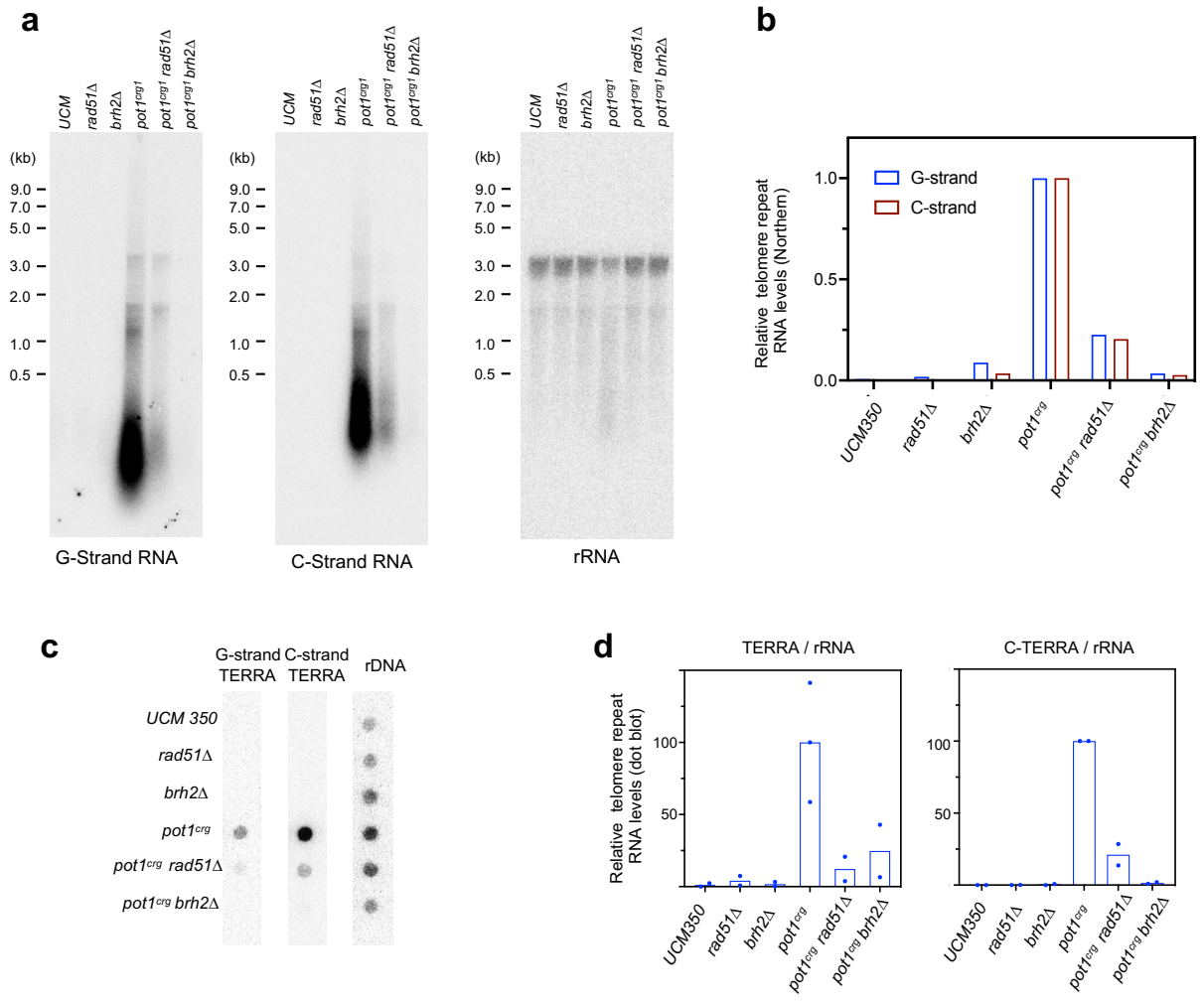

Figure 5. Telomere repeat-containing RNAs are elevated by pot1-deficiency and suppressed by *rad51*Δ and *brh2*Δ

a. RNAs from the indicated wild type and mutant strains grown in YPD were isolated by acid phenol extraction and subjected to Northern analysis using sequentially probes that detect G-strand repeats, C-strand repeats, and 26S rRNA.

b. The ratios of G- and C-strand RNA signals to the 26 rRNA signals from Northern analysis were calculated, and then normalized against the ratio of the *pot1*^{crg1} mutant and plotted. The normalized values for the *pot1*^{crg1} G- and C-strand RNA levels were each set to 100.

c. RNAs from the indicated wild type and mutant strains grown in YPD were isolated by acid phenol extraction, treated with Turbo DNase (Thermo Fisher Inc.), and subjected to dot blot analysis using sequentially probes that detect the G-strand repeats, C-strand repeats, and 26S rRNA.

d. The ratios of G- and C-strand signals to the 26 rRNA signals from Northern analysis (n = 2 or 3) were calculated, and then normalized against the ratio of the *pot1*^{crg1} mutant and plotted.